INTERNATIONAL JOURNAL OF
INTEGRATIVE AND
MODERN MEDICINE

Green Synthesis of Iron Oxide Nanoparticles Using Nutmeg Extract, Anti-Oxidant and Anti-Microbial Study

Muthanna C Urabee
Quality Assurance & Performance Evaluation Department, Mustansiriyah University, Baghdad, Iraq, muthannaorabi2810@uomustansiriyah.edu.iq

Mohammed I Sultan
Quality Assurance & Performance Evaluation Department, Mustansiriyah University, Baghdad, Iraq

Ahmed H Sadiq
Environmental Research Center, Technology University, Baghdad, Iraq

Abstract: This study presents the green synthesis of iron oxide nanoparticles (IONPs) using nutmeg (Myristica fragrans) extract as a reducing and stabilizing agent. The synthesis was optimized by varying reaction parameters including time, temperature, precursor concentration, extract-to-metal salt ratio, pH, and order of reagent addition. UV–Vis spectroscopy confirmed nanoparticle formation at λ_max = 365 nm, with optimal synthesis conditions determined to be 25 minutes at 30 °C, pH 9, and a 1:1 ratio of extract to iron chloride. The synthesized IONPs were characterized using FTIR, SEM, XRD, and Zeta potential analysis, revealing spherical nanoparticles of 45–53 nm, crystalline α-Fe_2O_3 structure, and moderate stability (zeta potential = −17.4 mV). Antioxidant activity assessed through DPPH assay showed strong radical scavenging by IONPs (85.98%) compared to nutmeg extract (79.08%) and standard Vitamin C (92.99%). Furthermore, antimicrobial tests indicated significant inhibitory effects of IONPs against Gram-positive and Gram-negative bacteria as well as Candida albicans. COX-2 enzyme inhibition assays demonstrated dose-dependent anti-inflammatory potential of both IONPs and nutmeg extract. These findings suggest that nutmeg-mediated IONPs exhibit promising biomedical applications due to their antioxidant, antimicrobial, and anti-inflammatory properties.

Keywords: Green synthesis, iron nanoparticles, nutmeg extract, Anti-oxidant, Anti-microbial

1. Introduction

Nanotechnology can be defined as the manipulation, measurement, and manufacturing of matter on an atomic level between 1-100 nm through certain chemical or physical processes to create materials with specific properties that can be used in various applications [1]. In the twenty-first century, Nano biotechnology is reflected as one of the most promising branches of science due to its attractive mode of action and wide applications in the field of biotechnology, chemistry, medicine, and material sciences [2]. Nanoparticles of iron oxides are one of the most widely used nanomaterials due to their easy synthesis and their ability to remove numerous substances, either alone or in combination with other adsorbents [3]. Plant extracts are a rich source of biomolecules, including both amines and phenols, which can act as metal reductants, very capable of electron loss and subsequent reduction of Fe^{2+} or Fe^{3+} to Fe^0 in aqueous solution [4]. Thus, this green approach could replace traditional toxic and complex physiochemical synthetic approaches for IONPs synthesis[5].

The phytochemicals such as carbohydrates, saponins, amino acids, flavonoids, terpenoids and proteins present in the plants extract play a key role in the synthesis of nanoparticles. One such valuable medicinal plant is *Myristica fragrans(nutmeg)* or commonly known as “nutmeg” which is an evergreen tree from the *Myristiceae* family [6]. Nutmeg consists of primary metabolites that form approximately 80% of dry nutmeg weight including lipids/fatty acids, carbohydrates, and proteins while approximately 20% of the nutmeg weight is comprised of essential oils (phenylpropanoids and

terpenes), phenolic compounds (caffeic, ferulic and protocatechuic acids, lignans/neolignans, and diarylalaknes), polyphenols and pigments (catechins, epicatechins, falvonoids, and cyanidins), Alkaloids, saponins as secondary metabolites [6],[7], and some minerals such as calcium, magnesium, iron, and potassium [8].

Cyclooxygenase-2(COX-2) is an enzyme involved in the production of prostaglandins, which are hormone-like substances involved in inflammation and pain signaling. It is one of two major isoforms of the cyclooxygenase enzyme, the other being COX-1 [9]. COX-2 is an inducible enzyme, meaning its production is typically low or absent in most tissues under normal conditions but can be increased in response to certain stimuli, such as inflammation, injury, or disease. It is primarily associated with the synthesis of prostaglandins that mediate inflammation and pain responses [10]. Cyclooxygenase 2 (COX-2) has been implicated in several physiological and pathophysiological processes including inflammation, tumor growth, and renal injuries [11].

2. Materials and Methods

2.1. Preparation of Nutmeg Extract

The nutmeg ethanolic extract was prepared by Abdulsattar *et al* [12]. Briefly, A mass of 14.28 grams of the crude powder of nutmeg seeds was refluxed with 100 ml of acetone (1:7) in the soxhlet apparatus for 8 hours to extract the bioactive compounds within the nutmeg dried seeds. Then the solution was filtered through a filter paper using Whatman Grade No.18 to eliminate residual solids and evaporated to dryness under vacuum at 40˚C. Afterwards, the dried extract was weighed and a stock solution of the extract was prepared by weighing one gram of dried extract and diluted with 1 ml of acetone then 9 ml D.W. in a 10mL volumetric flask to prepare $0.1 g.mL^{-1}$.

2.2. Green synthesis of Iron oxide nanoparticles

Ferric chloride hexahydrate ($FeCl_3.6H_2O$) was used as the precursor for the synthesis of α-Fe_2O_3 nanoparticles (IONPs). 50 mL of the nutmeg seeds extract was added dropwise with 50 mL of 0.1M $FeCl_3.6H_2O$ solution in a 1:1 ratio at room temperature. Following this, 1M NaOH was added till the pH became 11 as shown in scheme (2.2). The resultant mixture was stirred using a magnetic stirrer for 30 minutes and the formation of black colored solution confirmed the synthesis of IONPs. The nanoparticles were separated by centrifugation at 8000 rpm for 20 minutes and cleansed by subsequent washing with ethanol and water (2–3) times. The IONPs were finally dried in a hot air oven at 80 ℃ for 3 hours and stored in a seal-tight container for further use[12].

2.3. Optimization Study of IONPs

Various operation parameters effecting the formation of IONPs including reaction time ((0, 5, 10, 15, 20, 25, 30, 40, 50 and 60) minutes, temperature(10, 20, 30, 40, 50, 70 and 90)℃, concentration of iron chloride solution(0.05, 0.1, 0.2) M, concentration of ratio of extract to iron chloride solution (1:1, 2:1, 3:1, 1:2, and 1:3) , order of addition(Extract (E), Iron metal (M) and NaOH base (B)), pH (1, 2, 3, 4, 5, 7, 9, 11 and 12) were studied using a single factor experiments. Also, stability of the resultant solution was determined under optimized conditions, at an interval of 1 day, 1week, 2 weeks, 3weeks and 1 month. The absorbance of the resulting solutions was measured spectrophotometrically at λ_{max} = 365nm.

2.4. Characterization of IONPs

FTIR measurements: The dried IONPs and nutmeg seeds powder were analyzed by FTIR spectra by mixing with KBr and pressed to a plate for measurement, the spectrum was recorded in the range of (500-4000) cm^{-1}. **Zeta Potential Analysis:** An average of five measurements was taken. The size of IONPs was measured by electrophoretic light scattering (ELS) and dynamic light scattering (DLS) using Zeta Plus. **Scanning Electron Microscope (SEM) Analysis :** the SEM measurement was done to characterize the morphologies and shape of IONPs formed using a Hitachi SX-650 (Tokyo, Japan) at 20 KV of accelerating voltage. **X-Ray Diffraction (XRD):** The nanomaterial was deposited on a

piece of glass to be measured it using a Lab XRD 6000 Shimadzu XR-Diffraction. **Antimicrobial Activity (Comparison Studies)**

The antimicrobial activity were examined using agar diffusion method according to k. Ibrahim et al. [13]. Two Gram-negative bacteria (*Escherichia coli aureus*, and *Klebsiella sp*.), two Gram-positive bacteria (*Staphylococcus epidermis*, and *Staphylococcus aureus*), *and Candida albicans* (yeast) were used to be tested for the synthesized IONPs by nutmeg extract.

2.5. Free radical scavenging activity [14]

The antioxidant activity was measured using two different techniques spectrophotometric and microfluidic paper-based analytical device (μPADs)). Spectrophotometric procedure: 2 milliliters of each of prepared nano and plant extract (0.01 g mL-1) were added, indivtually to 2 milliliters of the DPPH (0.0094 %) and after 30 minutes of incubation at room temperature, the absorbance was measured at 517 nm against blank and the inhibition ratio was calculated. The second detection method was μPADs: the fabrication of the paper was done according to Peters *et al* [23]procedure. 5 microliters of each of the prepared concentrations was added to 5 microliters of the DPPH to the different detection circular reaction zone to prepare the blank. Afterwards, the detection circular reaction zone was left to dry at room temperature. Then, a picture was taken using a Samsung note 9 mobile phone to be entered into the image J program for absorbance readers.

2.6. Determination of Total Phenolic Compounds

Total phenolic content of nutmeg seed extract was determined using the Folin–Ciocalteu method [15], with gallic acid as the standard. Briefly, 100 μL of the extract (0.1 g mL^{-1}) or standard solution (0.00312–0.1 mg mL^{-1}) was mixed with 1 mL of 10% Folin–Ciocalteu reagent. After 3 min, 3 mL of sodium carbonate solution (2 g 100 mL^{-1}) was added, and the mixture was incubated at 25 °C for 2 h. Absorbance was measured at 760 nm against a reagent blank. Total phenolic content was expressed as mg gallic acid equivalents (GAE) per g extract.

2.7. Statistical Analysis

The results were analyzed statistically using the Statistical Package for Social Sciences computer program version 22.0 (IBM SPSS Statistic software, IBM Corporation, New York, United States). Data were analyzed using descriptive statistics of the SPSS software. The values were expressed as mean ± standard deviation (SD), coefficient variation (CV).

3. Results and Discussion

Iron nanoparticles were synthesized using nutmeg acetone extract prepared by Abdulsattar *et al.*[12] due to the presence of various phytochemicals such as polyphenols, flavonoids, glycosides, and tannins that act as reducing and stabilizing agents for the synthesis of nanoparticles (NPs) [16]. The qualitative evidence for IONPs formation was the color change from yellow to brown. The quantitative proof was done by UV–Vis absorption spectra analysis of IONPs (Figure 1) that gave an increase in the absorbance of λ_{max} = 365 nm. This is due to the reduction of ferric to Fe-NPs by the reactive functional moieties present in nutmeg extract. The color change is a result of the excitation in the UV–vis spectrum depending on the amount of the NPs. IONPs shows the highest absorption band peak, while the absorption band of extract and salt were less than it. The absorption bands of IONPs have been reported within the range of (250–400) nm by Bashir A. *et al*. [17].

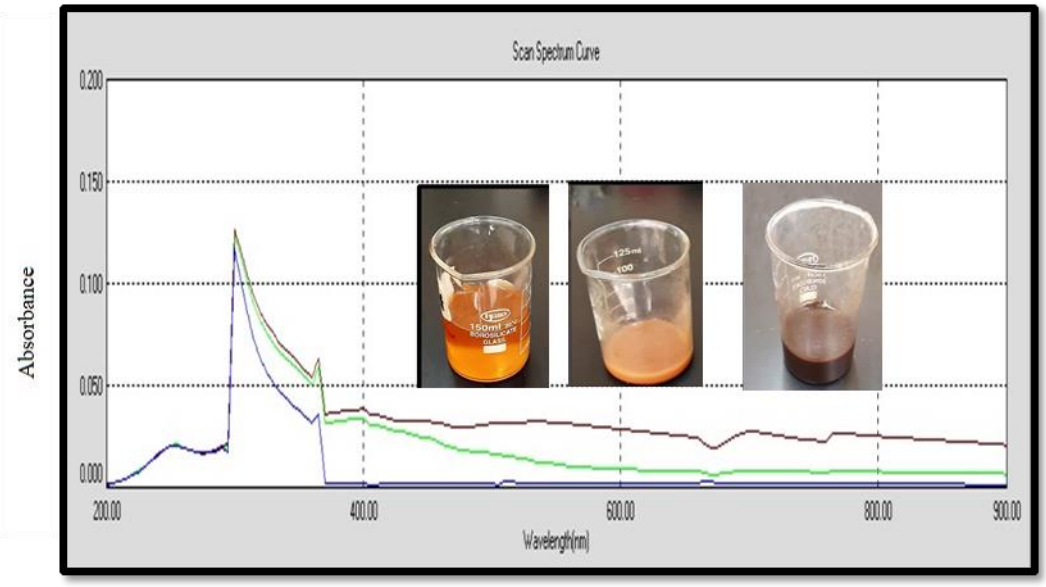

Figure 1: UV-Visible absorption spectrum of nutmeg extract, iron salt and IONPs, (red = IONPs, green= nutmeg extract, blue= $FeCl_3$ solution), insert in the figure from the left a consecutive images of $FeCl_3$ solution, Nutmeg extract solution, and IONPs solution showing the green synthesis of IONPs.

The phytochemicals react with the iron ions to give IONPs, as it is prone to oxidation, rather than reducing Fe^{+3} to Fe^0 [18]. The development of Fe_2O_3 nanoparticles can be explained by the chemical reactions concerned and the crystal growth behaviours of iron oxide. The synthesis of IONPs was performed using ferric chloride ($FeCl_3$) and NaOH. NaOH maintains the pH value as well as bringing hydroxyl ions to the solution. The $FeCl_3$ reacts with NaOH and forms FeO(OH) according to the chemical reactions (1-3).

$$FeCl_3 + {}_3NaOH \rightarrow Fe(OH)_3 + {}_3NaCl \quad (1)$$

$$Fe(OH)_3 \xrightarrow{Plant\ Extract} Fe_3O_4 + 3H_2O \quad (2)$$

$$2Fe(OH)_3 \xrightarrow{Plant\ Extract} Fe_2O_3 + 3H_2O \quad (3)$$

[19].

3.1. Optimization Study of IONPs Synthetic Conditions

The effect of time was studied over the time interval from (0-60) minutes that is required for the completion of the reaction. As can be seen from (figure 2 a, and b), the increase of time lead to a gradual increase in IONPs absorbance and gave the highest value at 25 minutes which indicated the increased concentrations of the IONPs. Afterwards, there was a plateau decrease in absorbance until 60 minutes. Therefore, the optimum time required for the formation of IONPs was 25 minutes and was recommended for further experiments. The influence of different temperatures ranging from (10-90) $^{\circ}$C was studied and measured at λ_{max} = 365nm. It can be seen from (Figures 3 a, and b) there was a plateau increase of absorbance intensity for different temperatures. Therefore 30°C (room temperature) was chosen as optimum temperature and considered adequate for IONPs development and formation. Karade *et al.* found that the magnetic measurements proved the super paramagnetic behaviour of NPs with a non-saturating MS value of 8.5 emu/g at room temperature (300K). Further, the hyperthermia study reveals, the NPs achieved a temperature of 40 $^{\circ}$C and 43 $^{\circ}$C within 6 min and reaches up to 43 $^{\circ}$C and 45 $^{\circ}$C within 10 min only for 5 $\mu g.mL^{-1}$ and 10 $\mu g.mL^{-1}$ concentrations, respectively [20]. The absorbance of IONPs affected by different concentrations of ferric chloride ranged between (0.05–0.2) M was studied and measured at a maximum wavelength of 365 nm and results revealed that 0.1M gave the best absorbance intensity. Further increase in iron concentration made a drop in absorbance intensity (figure 4 a, and b). As a result, 0.1M was selected as the optimum salt concentration and used

for further experiments. The ratio between the ferric chloride solution and nutmeg extract solution was studied using different ratios of both solutions. As can be seen from Figure 5, the optimum absorbance was obtained at a 1:1 ratio for iron and nutmeg extract. It is clear that when the iron concentration going to be equal to the extract solution the absorbance has its highest value, but when the amount of iron increases the stability has decreased, it is maybe due to the amount of extract no longer being enough to reduce all the iron amount [21]. Due to the significant impact of pH change on the IONPs synthesized reaction, experiments were done to show the effect of pH in the range of 1 to 12 using NaOH and HCl buffer solutions. As can be seen from figure 6, pH 9 gave the highest absorbance at a maximum wavelength. A decrease in absorbance was observed can be attributed to the iron ions in iron hydroxyl species which affect the reaction [18]. Therefore, pH 9 was selected as the optimum pH. The effect of varied sequences of reagents addition including extract (E), iron metal (M) and NaOH base (B) on maximum absorbance intensity were tested as shown in figure 7. The data obtained revealed that the addition of nutmeg extract, iron metal and base gave the highest absorbance intensity (0.501).

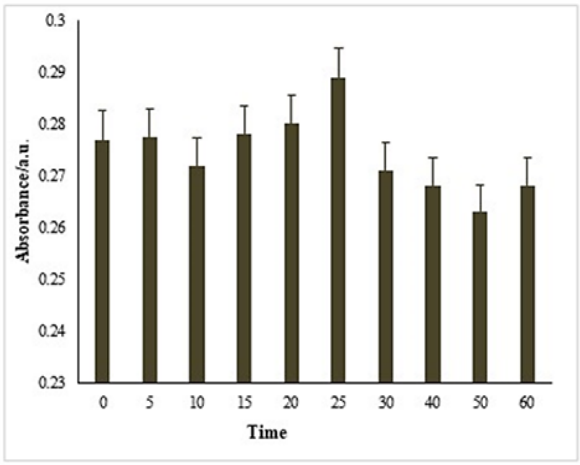

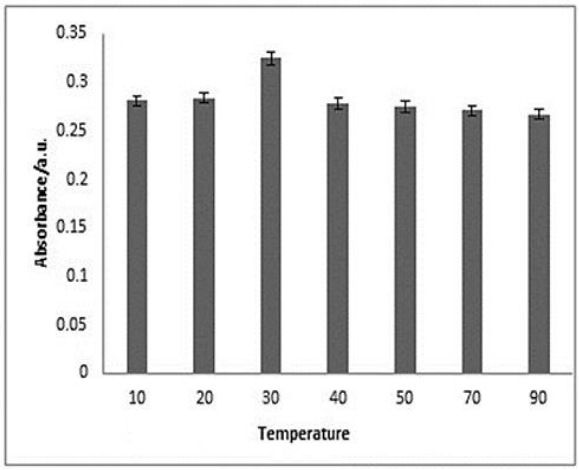

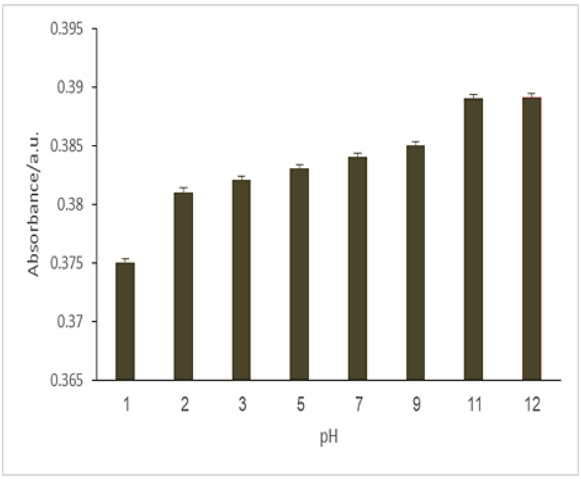

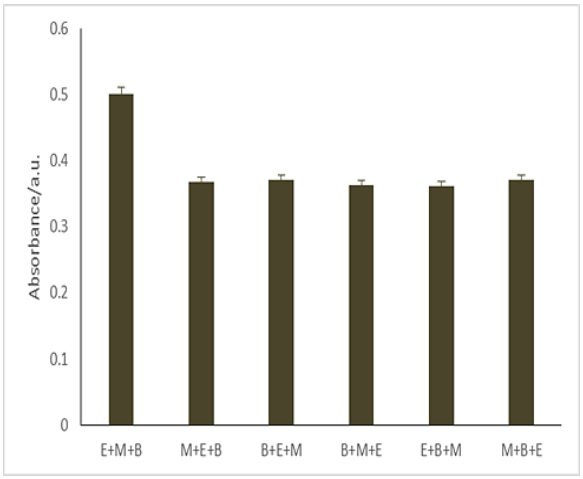

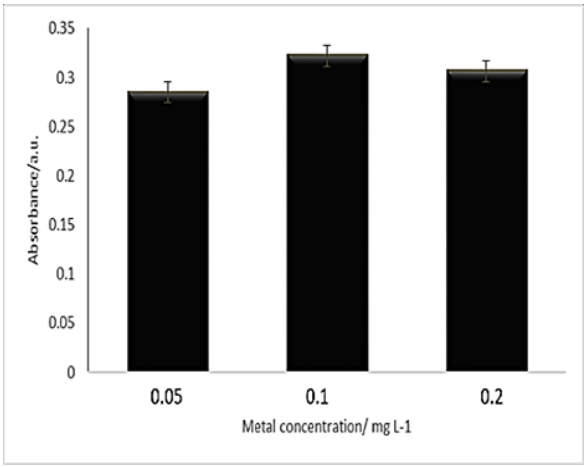

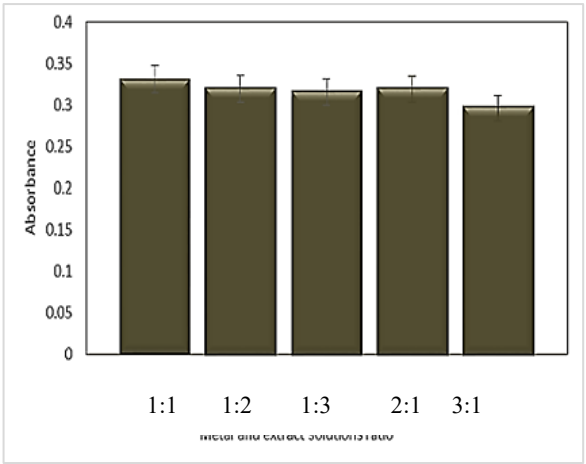

Figure 2: Extraction yield percentage of the optimized extraction system parameters. a) Reaction time, b) temperature, c) pH, d) order of addition, e) Concentration of FeCl3, f) ferric chloride and nutmeg extract ratio

Where: (a) extraction solvent (BMIMCl, ethanol , deionized water, ethyl acetate), b) extraction techniques (maceration, ultrasound, digestion, and Soxhlet), c) extraction time ranging from (5-90) minutes, d) temperature (25, 50, 75,100) °C, e) pH ranging from (2-9), f) liquid to solid (15 mL: 0.5 g, 15 mL:1 g, 15 mL:1.5 g), g) solid to liquid ratio (0.5 g: 5 mL, 0.5 g: 10 mL, 0.5 g: 15 mL, 0.5 g: 20 mL, 0.5 g: 40 mL).

3.2. Stability Study

The stability of interaction time for the realization of IONPs by the reaction between iron ion and the reducing material in the nutmeg extract was investigated for one month from synthesis. Figure 8 shows that the synthesized IONPs product was stable for one week indicating good stability of biosynthesized IONPs.

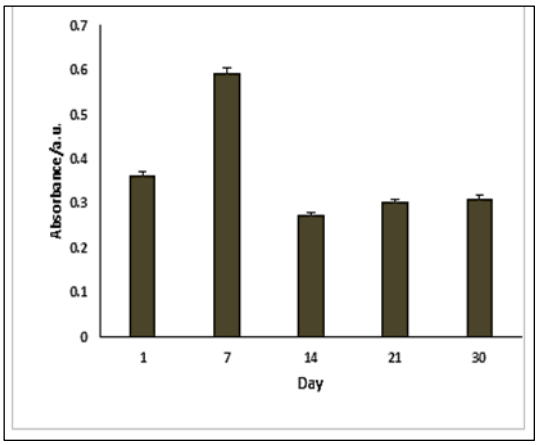

Figure 3: Effect of stability time over the time interval from (1-30) days on absorbance intensity.

3.3. Characterization of IONPs

The FTIR chart (400-4000) cm^{-1} of the plant extract (figure 4 a) confirm the existence of various reducing agents functional groups presents in the plant extract while IONPs chart (figure 4 b) confirm the synthesis of IONPs. The difference between the spectra could be considered as proof of the transformation. The Fe-O bond was definite by the presence of peaks at 474.49 cm^{-1}, 621.08 cm^{-1} and 678.94 cm^{-1} [200][201]**.** The peaks at the position of 3357.57 cm^{-1} represent the –OH bond stretching from the aqueous phase. In addition, the peaks at 1433.11 cm^{-1}, and 3691.57 cm^{-1} represents the –OH bond stretching and bending from various phenolic and carboxylic groups respectively [202]. Furthermore, the peaks at 2927.94 cm^{-1}, 1625.99 cm^{-1} and 1101.35 cm^{-1} denotes C–H stretching, C=C stretching and C–O stretching ensuring the presence of alkane, conjugated alkene and secondary alcohol in the plant extract as observed by a previous study***[22]***. The shift or absence in peaks position observed in IONPs chart indicate that these functional groups are involved in the bioreduction of iron ions into iron oxide nanoparticles. Wisam *et al*. cleared that FT-IR spectra of the (β-Fe_2O_3) NPs have a strong absorption at 526 cm^{-1} were assigned to the band vibrations of FeO [23]. It has been noted that, in the FTIR spectra of iron oxide nanoparticles, the bands observed between (400-570) cm^{-1} have been evaluated magnetite while maghemite has been recorded between (620660) cm^{-1} and the bands on 470 cm^{-1} and 540 cm^{-1} are considered as hematite. In the recorded IR spectrum (figure 3.13), the bands recorded in 470 cm^{-1}, 501 cm^{-1}, 555 cm^{-1}, 594 cm^{-1} and 633 cm^{-1} could be the different forms of iron oxide nanoparticles[24].

The morphology of IONPs was monitored by SEM analysis and the particle size was found in the range of (45–53) nm, the particles were of a nano-range size, semi-spherical shape and in agglomerated form as shown in figure 5. The adopted green route furnished IONPs in the surface of NPs is smooth with good crystallinity, in agreement with other studies [25]. The particles dispersed

and hexagonal single crystals shape with particle size (54nm) appeared [26][27]. Bhuiyan, Md. *et al*. found that the morphology of IONPs was monitored by SEM analysis and the particle size was found in the range of (25–55) nm, the particles were of variable shapes and in agglomerated form. The agglomeration of agglomerated might be due to the presence of biological compounds on the surface of particles. Due to H-bonding present in bioactive molecules, the particles appeared to be in the form of aggregates [28].

The value of the zeta potential measurement means that the produced iron oxide nanoparticles are potentially stable. Increasingly, particle repulsion is the bigger the positive or negative zeta potential value. Stable nanoparticles prevent and maintain nano-scale flocculation and aggregation of particles. Zeta potential was shown to have an average zeta potential for iron oxide nanoparticles of -17.4 mV (figure 6), demonstrating the stability of the colloid iron oxide. The incipient instability of the nanoparticles generally occurs in the colloid ±10 to ±30. Kanagasubbulakshmi, S. *et al*. found that the z-potential of initial magnetic fluid was -40.9 mV and of modified IONPs was in the range from (-35 to -48) mV, indicating relative good stability of all prepared IONPs [29].

Crystallized peaks were observed without impurities with major diffraction peaks at 2θ values of 22.9 (012), 34.5 (104), 35.5 (110), 50.9 (024), 58.8 (018), 62.9 (214), and 64.6 (300) degrees. After calcination at 400 ºC shows the formation of α-Fe_2O_3**,** based on comparing their XRD patterns with the standard pattern of α-Fe_2O_3 (JCPDS 33-0664). The first peak belongs to the extracted fiber inside the sample.

$$\boldsymbol{D = K\lambda / \beta \cos \theta} \quad (1)$$

The crystallite size is determined using the Debye–Scherer's formula (Eq. 1) where D is the crystallite size (nm), K is a constant with value (0.9), the X-rays wavelength λ=0.15406 nm, β is the full width at half maximum (FWHM) intensity measured in radians, and θ is the Bragg diffraction angle of the plane ***[22]***. Viju K. *et al*. found that The green synthesized iron oxide nanoparticles, distinct peaks were found at (32.11, 35.89, 43.65, 56.88, 62.97°) accounting for crystal planes (220), (311), (400), (510), and (440) respectively[30]. Ismat B. *et al.* found that the peaks observed in XRD analysis revealed the spinal structured magnetite and exhibiting peaks at 2 theta values of 30.60, 35.21, 42.13, 53.53, 57.6 and 63.01, which corresponds to diffraction planes of 220, 311, 400, 422, 511 and 440, respectively [208]. The XRD data as shown in figure 11 indicates that the crystal planes of (012), (104), (110), (024), and (116) correspond to the of 22.16, 35.5, 36.53, 40.64, 49.57, and 57.08, indicates the formation of α-Fe_2O_3 nanoparticles. The intense and sharp peaks undoubtedly revealed that α-Fe_2O_3 nanoparticles formed by the reduction method using nutmeg extract were crystalline. The results are almost similar to the results obtained for iron oxide nanoparticles by other researchers [17][31][32].

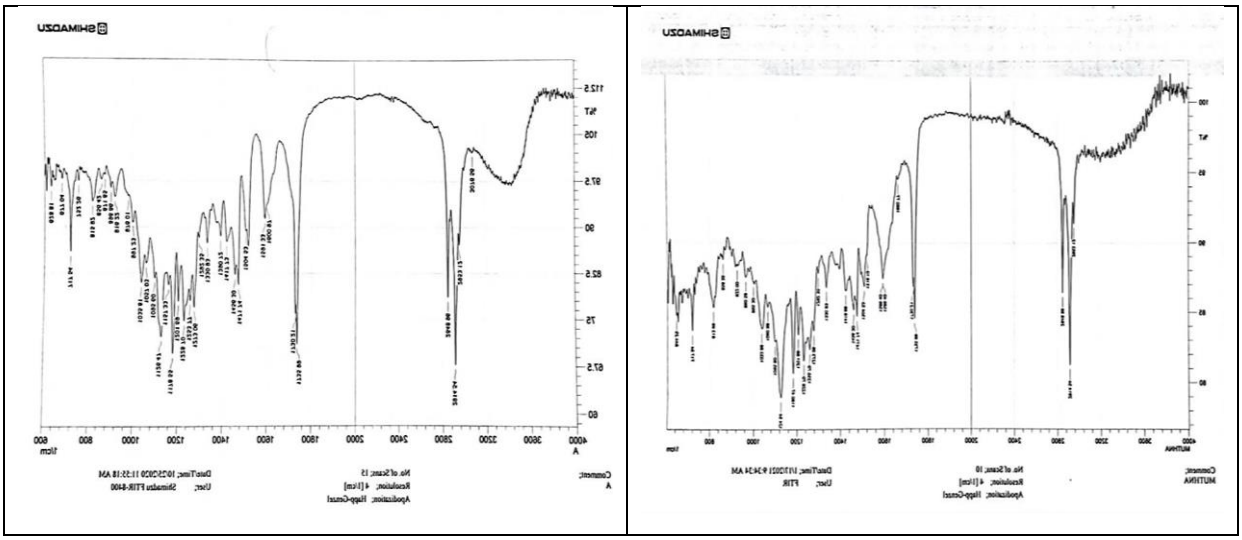

Figure 4: (a) The FTIR chart for nutmeg extract, (b) The FTIR chart for the synthesized IONPs.

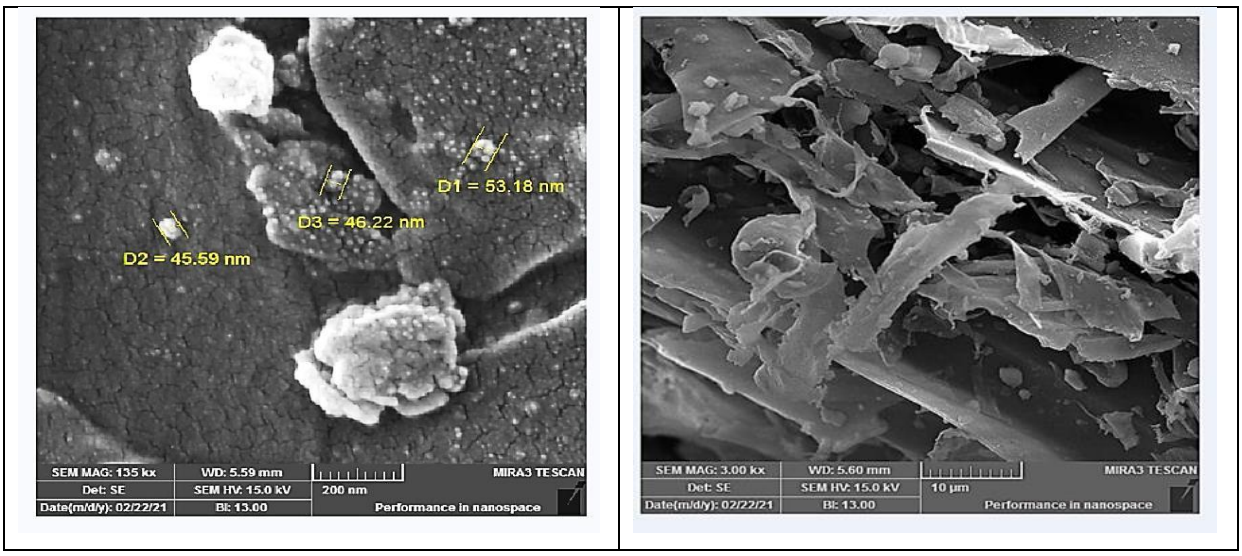

Figure 5: SEM images of IO NPs (Left=200 nm, Right=10 µm).

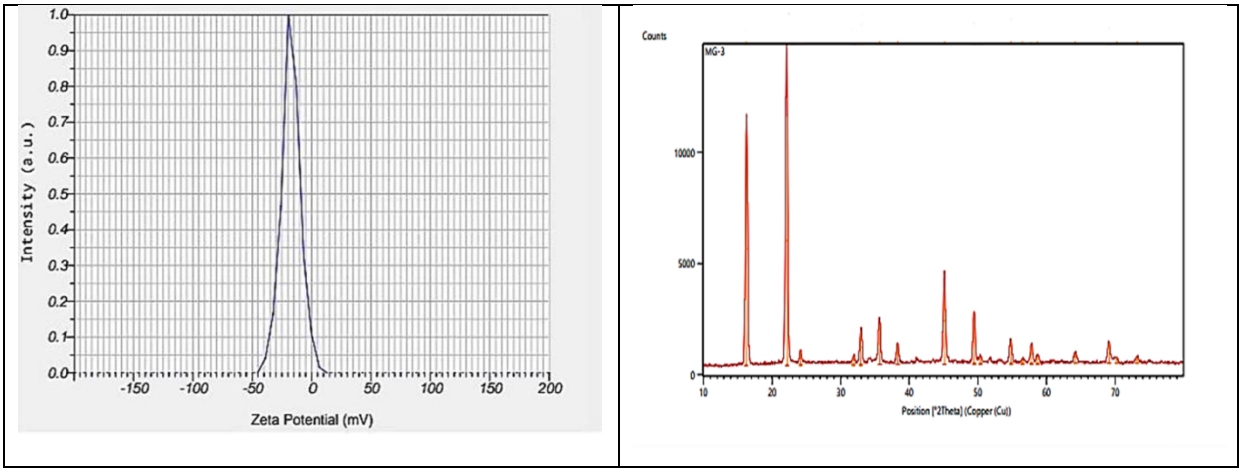

Figure 6: (a) Zeta potential distribution chart of IONPs, (b) XRD pattern of Synthesized Iron oxide Nanoparticles.

3.4. Total Phenolic Contents

Preliminary investigations were done to determine total phenolic compound and free radical scavenging activity using a novel, easy-to-use, a cost-effective and simple technique called microfluidic paper-based analytical device (µPADs) which is considered as an alternative to conventional thin-layer chromatography (TLC) technique towards the construction of a platform that can use routine analysis outside centralized laboratories. Folin–Ciocalteu reagent was used and the greyish color was observed after the addition of extract and IONPs to Folin–Ciocalteu reagent and 2% Na_2CO_3, as can be seen in figure 5 indicating a good phenolic content compared with standard Gallic acid.

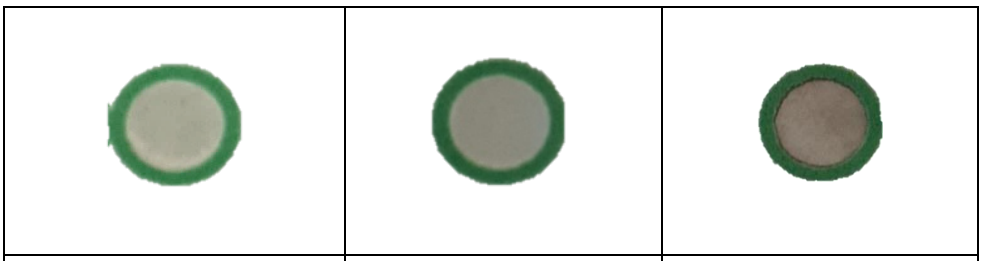

(a)Standard Gallic acid | (b)Nutmeg extract | (c)IONPs

Figure 7: µPADs images for (a) standard Gallic acid, (b) Nutmeg extract, and (c) IONPs.

The total phenolic contents were calculated using the standard curve of gallic acid, acetone nutmeg extract and IONPs as shown in figure7 and were found to be (0.964, and 0.6217) $mg.mL^{-1}$ for acetone nutmeg extract and IONPs, respectively which indicate the high phenolic levels in synthesized IONPs than acetone extracts. In addition, the results revealed that total flavonoids were higher in plant-IONPs compared to those found in the extract alone. This can be related to the extraction of both nonpolar and semipolar soluble phenolic acids. Compounds such as phenolics, flavonoids, terpenoids, and soluble proteins have been reported to act as capping agents [33]. It is suggested that the phenolic compounds, which are antioxidants, are responsible for the antibacterial activity. Jinous et al, found that the commonly known phytochemical compounds of nutmeg are volatile substances, terpenoids, phenolics, lignin compounds, protein, mucilage and starch [34].

Table1: Total phenolic of nutmeg acetone extract.

Concentration (Gallic acid) $mg.mL^{-1}$	**Absorbance**	**Total phenolic content in Nutmeg extract $mg.\ mL^{-1}$**
0.2	0.019	-
0.4	0.050	-
0.6	0.063	-
0.8	0.075	-
1	0.084	-
Extract	0.081	0.9640
IONPs	0.060	0.6217

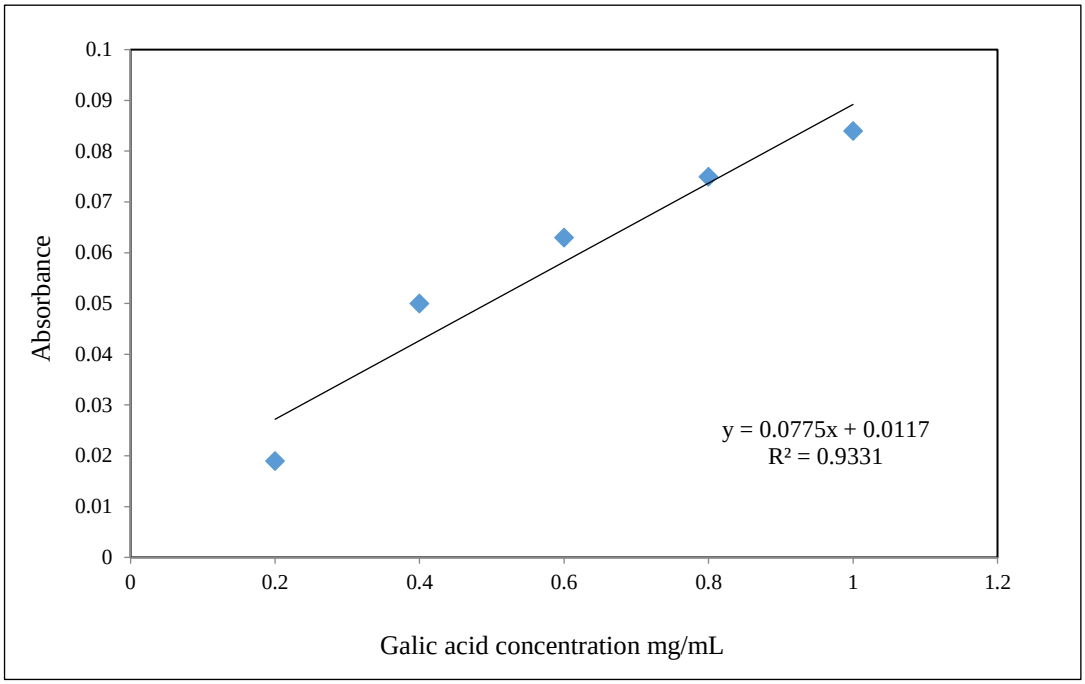

Figure 8: Total phenolic concentration of nutmeg acetone extract.

3.7 Free Radical Scavenging Activity

Qualitative determination of standard vitamin C, nutmeg extract, and IONPs radical scavenging was done against DPPH radical using the microfluidic paper-based analytical device (µPADs). The greyish color for nutmeg extract and IONPs as can be seen in figure (9) indicate a good activity of the extract and IONPs against the DPPH compound, while standard vitamin C indicated a less scavenging activity.

		
(a)Standard Vitamin C	(b)Nutmeg Extract	(c)IONPs

Figure 9: µPADs images for (a) Standard Vitamin C, (b) Nutmeg Extract, and (c) IONPs.

The antioxidant activity of synthesized IONPs and acetone nutmeg extract was determined by using DPPH free radical assay. The higher DPPH scavenging effect (%) value was in Vitamin C. 92.99%, then in IONPs 85.98 %, and lastly in nutmeg extract 79.08 %. The effect of different concentrations of IONPs and nutmeg extract on DPPH radical antioxidant activity is shown in (table2 and table3). Our results revealed that the nutmeg extract and synthesized IONPs are free radical scavengers. However, the IONPs exhibited more scavenging activity of DPPH than nutmeg extract. The DPPH activity of the IONPs and nutmeg extract was found to increase in a dose-dependent manner[35].

The high antioxidant capacity of seed extract is due to the quite high presence of tannin, flavonoids and terpenoids compounds. These compounds contribute to extracted antioxidants to serve as electron donors. The basic structure of flavonoids is the two hydroxyl groups attached to the benzene ring. Both hydroxyl groups act as an electron donor group and may increase antioxidant activity. This preliminary study indicates the interesting anti-oxidative stress activity of nutmeg extract suggesting its promising applications as a medicinal source for the treatment and prevention of free radicals associated diseases. The DPPH radical scavenging activity indicated percent free radical scavenging ranged from (40.78% to 11.48%) from (400 to 25) $\mu g.mL^{-1}$, as indicated in (figure 3.19). IONPs also revealed total antioxidant capacity (TAC) and total reducing power potential (TRP) calculated as µg AAEs/mg. At

the highest concentration of 400 µg.mL-1, TRP was revealed as 251 µg AAEs/mg and 38.23 µg AAEs/mg [36]. As a result of the DPPH test, it has been calculated that 1 gram of nanoparticles has antioxidant activity equivalent to 5.14 mg ascorbic acid. In addition, it was shown that the nanoparticle at a concentration of12.118 $mg.mL^{-1}$ has an antioxidant capacity that can destroy half of the DPPH radicals in the environment. In other words, we can say that the SC50 value calculated as a result of the DPPH test for the nanoparticle is 12.118 $mg.mL^{-1}$. The scavenging efficiency of DPPH radicals of 3 different iron oxide nanoparticles obtained by green synthesis from palm leaf was found between 2 and 26.4 $mg.mL^{-1}$ [37].

Table2: Determination of DPPH free radical for nutmeg extract.

The concentration of the extract (mg.mL-1)	DPPH Scavenging effect (%)	DPPH scavenging effect (%) Mean ± SD
Vitamin C	92.99	92.88 ± 0.08
0.00312	11.13	11.11 ± 0.01
0.00625	57.63	57.53 ± 0.06
0.01250	74.59	74.43 ± 0.11
0.02500	77.91	77.82 ± 0.07
0.05000	78.27	78.31 ± 0.03
0.10000	79.08	79.07 ± 0.02

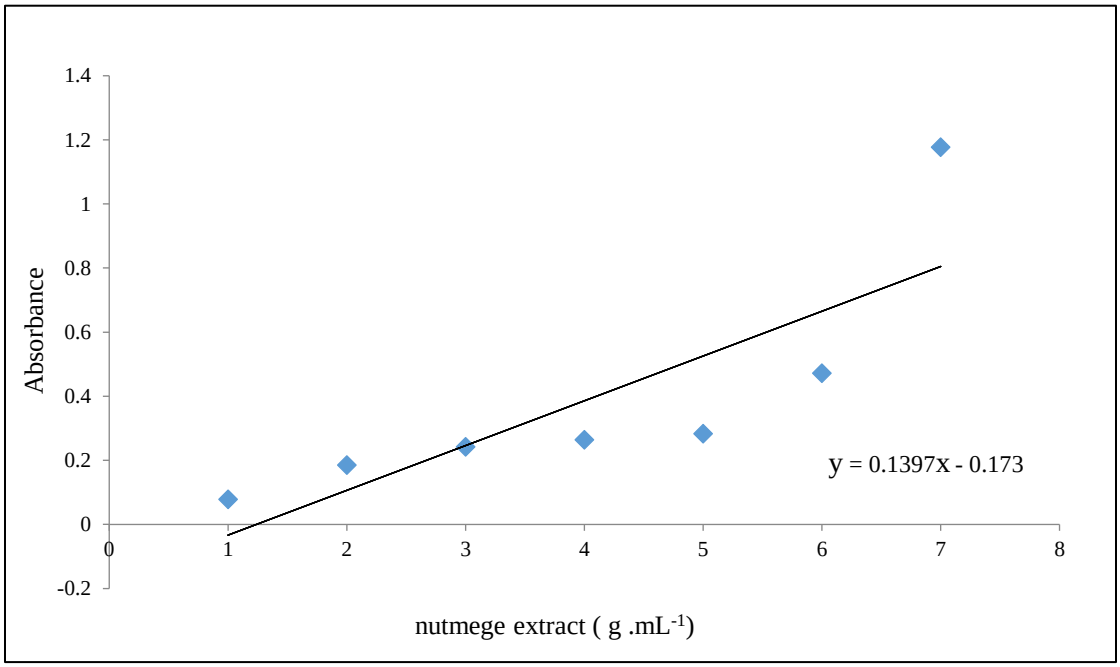

Figure 10: Free radical scavenging activity of nutmeg acetone extract.

Table3: Determination of DPPH free radical for IONPs.

The concentration of the IONPs (mg.mL^{-1})	DPPH Scavenging effect (%)	DPPH scavenging effect (%) Mean ± SD
Vitamin C	92.99	93.50 ± 0.41
0.00312	15.01	15.17 ± 0.61
0.00625	60.55	61.37 ± 0.57
0.01250	77.34	77.71 ± 0.61
0.02500	80.56	80.04 ± 0.44
0.05000	82.11	82.04 ± 1.48
0.10000	85.98	85.50 ± 1.46

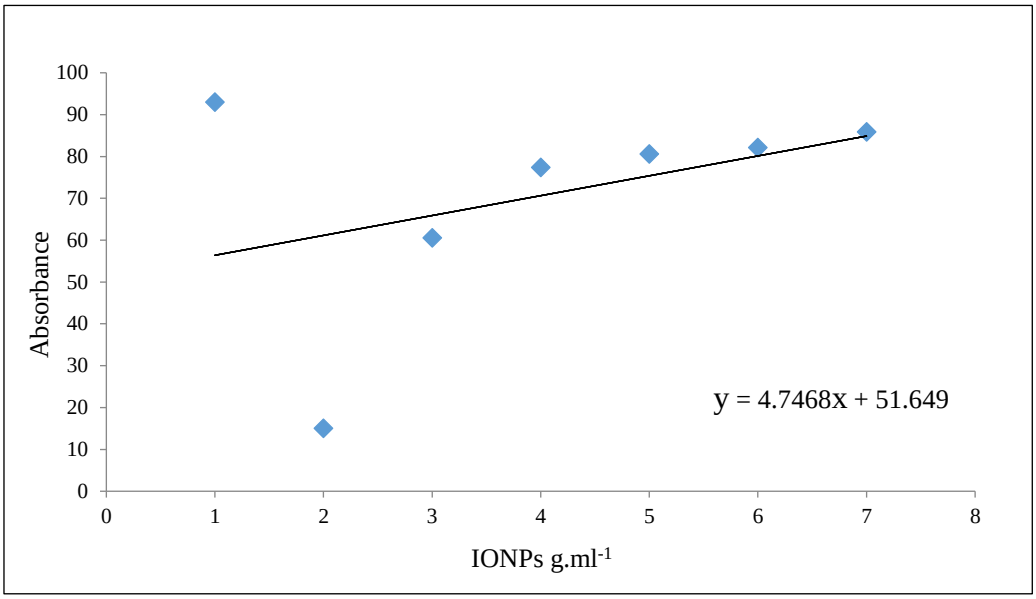

Figure 11: Free radical scavenging activity of IONPs.

3.9 Antimicrobial Activity Comparative Studies

Acetone, methanol nutmeg seeds extracts and IONPs were subjected for their antimicrobial activity. Preliminary screening against *Staphylococcus aureus*, *Staphylococcus espidermidis, Escherichia coli, Klebsiella sp.* as well as *Candida albicans* was performed. Acetone extract at the concentration of 0.1 mg.mL^{-1} (S7) showed an effect against all test microorganisms. Overall, Candida albicans, was the most affected microorganism as listed in (Table 4) while the methanol extract showed no effect against tested microorganisms as shown in (Table 5).On the other hand, the synthesis nanoparticles showed increasing antibacterial properties as shown in (Table 6).

Table4: Mean and standard deviation (SD) values of acetone extract from seeds of nutmeg against *Staphylococcus aureus, Staphylococcus epidermidis, Escherichia coli, Klebsiella sp.* and *Candida albicans*.

Sample No.	Gram-positive		Gram-negative		Fungi
	S.aureus	***S. espidermis***	***E .coil***	***Klebsiella sp.***	***C.albicans***
	Mean ± SD	**Mean ± SD**	**Mean ± SD**	**Mean ± SD**	**Mean ± SD**
S1	-	-	-	-	-
S2	-	-	-	-	10.33 ±1.24
S3	7.33 ± 0.47	-	-	-	-
S4	8.66 ± 1.24	-	-	-	11.66 ± 1.24
S5	-	-	-	-	11 ± 0.81
S6	-	-	-	-	12.33 ± 0.47
S7	11.6 ± 0.47	12 ± 0.81	14 ± 0.81	11.33 ± 1.24	13 ± 1.63

Table5: Mean and standard deviation (SD) values of methanol extract from seeds of nutmeg against *Staphylococcus aureus, Staphylococcus epidermidis, Escherichia coli, Klebsiella sp.* and *Candida albicans*.

Sample No.	Gram-positive		Gram-negative		Fungi
	S.aureus	***S. espidermis***	***E .coil***	***Klebsiella sp.***	***C.albicans***
	Mean ± SD	**Mean ± SD**	**Mean ± SD**	**Mean ± SD**	**Mean ± SD**
S1	-	-	-	-	-
S2	-	-	-	-	-
S3	-	-	-	-	-
S4	-	-	-	-	-
S5	-	-	-	-	-
S6	-	-	-	-	-
S7	-	-	-	-	-

Table6: Mean and standard deviation (SD) values of IONPs against Staphylococcus aureus, Staphylococcus epidermidis, Escherichia coli, Klebsiella sp. and Candida albicans.

Sample No.	Gram-positive		Gram-negative		Fungi
	S.aureus	***S. espidermis***	***E .coil***	***Klebsiella sp.***	***C.albicans***
	Mean ± SD	**Mean ± SD**	**Mean ± SD**	**Mean ± SD**	**Mean ± SD**
S1	-	12.6 ± 1.69	12.33 ± 1.24	-	-
S2	-	-	11.66 ± 1.24	-	-
S3	11.3 ± 0.47	-	10.80 ± 0.84	-	-
S4	13 ± 0.81	-	11.16 ± 1.31	-	-
S5	14.3 ± 1.24	-	-	-	-
S6	-	-	-	-	-
S7	17.6 ± 1.24	25.6 ±1.69	16.33 ± 1.24	14.66 ± 1.69	24.66 ± 1.24

There are different inhibition mechanisms against microorganisms such as cell membrane damage, inhibition of protein synthesis and disruption of cell biological functions and cell membranes by specific enzymes. The nature of bacterial cell wall is influenced by the presence of compound like α-Pinene and β-pinene (pinene-type monoterpene hydrocarbons) which is involved in the membrane cell

wall disruption by the lipophilic compounds [38]. In addition, the nature of gram-negative bacteria cell walls with high lipid content (up to 20 %) compared with 02% for gram-positive is responsible for the resistance of microorganisms such as Escherichia coli [13]. While gram-positive bacteria show more sensitivity to the antimicrobial compounds found in nutmeg [39]. On the other hand, there are several hypotheses involved to explain the extracting mechanism of NPs against bacterial strains. Generally, the iron oxide nanoparticles showed their antibacterial properties due to the production of reactive oxygen species (ROS), oxidative stress caused by ROS, the reaction of ions released by nanoparticles with thiol groups (–SH) of the bacterial cell, therefore, interrupting the DNA replication and protein synthesis process of microorganism by altering their structure [40]. Again, the positively charged metal ions released from NPs might interact with negatively charged bacterial strains surface with resulting in the disruption and destabilization of microorganism surface protein and subsequent cell death [12]. Alcoholic extracts of nutmeg showed antibacterial activity against micrococcus pyogens var. aureus [41]. Essential oil of nutmeg caused a significant inhibition of the growth and survival of Yersinia enterocolitica and Listeria monocytogenes [42]. It has been found that methanol extract of M. fragrans (seed), having a MIC of 12.5 µg.mL-1 against H. pylori strains, is highly effective in the treatment of gastrointestinal disorders[43].

It is concluded that nutmeg acetone extract has antimicrobial activity against gram-positive bacteria in contrast to gram-negative bacteria which are resistant to both acetone and methanol extracts. While Candida albicans showed a higher sensitivity to acetone extract ranging from 11 to 15 mm diameter. For IONPs, the antibacterial activity increased in the range of 14 mm diameter.

4. Conclusion

The present study successfully demonstrates the environmentally friendly synthesis of iron oxide nanoparticles using nutmeg extract as a green reducing and stabilizing agent. Optimal synthesis was achieved under mild conditions (25 minutes, 30°C, pH 9) resulting in stable, semi-spherical α-Fe_2O_3 nanoparticles with sizes ranging between 45–53 nm. Comprehensive characterization confirmed their crystalline structure and surface chemistry. The IONPs exhibited superior antioxidant activity (85.98%) compared to the raw extract (79.08%), as well as effective antimicrobial action against various bacterial and fungal strains. Additionally, both the nutmeg extract and synthesized IONPs significantly inhibited COX-2 activity, highlighting their potential anti-inflammatory properties. The results underscore the therapeutic and environmental advantages of using nutmeg in the green synthesis of nanomaterials, opening pathways for further exploration in biomedical and pharmaceutical applications.

Acknowledgments

The authors would like to thank Mustansiriyah University, Baghdad, Iraq (www.uomustansiriyah.edu.iq) for their help in completing this work.

Data Availability: None.

Conflict of Interest: The authors declare that they have no conflict of interest.

Competing interests: The authors declare that they have no competing interests.

Funding Information: No funding was received for conducting this study.

Author's Contribution: Muthanna contributed to the study design and idea. Muthanna, Ahmed, and Mohammed carried out the experimental work, data collection and data analysis. Muthanna and Mohammed contributed to the results discussion, writing, drafting and editing of the paper. All of the authors checked and approved the overall manuscript, and approved the final version of the manuscript.

References

1. G. KSV, "Green Synthesis of Iron Nanoparticles Using Green Tea leaves Extract," J. Nanomedine. Biotherapeutic Discov., vol. 07, no. 01, pp. 1–4, 2017, doi: 10.4172/2155-983x.1000151.
2. S. Balakrishnan, I. Sivaji, S. Kandasamy, S. Duraisamy, N. S. Kumar, and G. Gurusubramanian, "Biosynthesis of silver nanoparticles using Myristica fragrans seed (nutmeg) extract and its antibacterial activity against multidrug-resistant (MDR) Salmonella enterica serovar Typhi isolates," Environ. Sci. Pollut. Res., vol. 24, no. 17, pp. 14758–14769, 2017, doi: 10.1007/s11356-017-9065-7.
3. A. C. De Lima Barizão, M. F. Silva, M. Andrade, F. C. Brito, R. G. Gomes, and R. Bergamasco, "Green synthesis of iron oxide nanoparticles for tartrazine and bordeaux red dye removal," J. Environ. Chem. Eng., vol. 8, no. 1, p. 103618, 2020, doi: 10.1016/j.jece.2019.103618.
4. Y. Liu, X. Jin, and Z. Chen, "The formation of iron nanoparticles by Eucalyptus leaf extract and used to remove Cr (VI)," Sci. Total Environ., vol. 627, pp. 470–479, 2018.
5. X. Jin, Y. Liu, J. Tan, G. Owens, and Z. Chen, "Removal of Cr (VI) from aqueous solutions via reduction and absorption by green synthesized iron nanoparticles," J. Clean. Prod., vol. 176, pp. 929–936, 2018.
6. N. Naeem, R. Rehman, A. Mushtaq, and B. Ghania, "Nutmeg: A review on uses and biological properties," Int. J. Chem. Biochem. Sci., vol. 9, no. October, pp. 107–110, 2016, [Online]. Available: https://www.researchgate.net/publication/336825717_Nutmeg_A_review_on_uses_and_biological_properties
7. Jinous Asgarpanah, "Phytochemistry and pharmacologic properties of Myristica fragrans Hoyutt.: A review," African J. Biotechnol., vol. 11, no. 65, 2012, doi: 10.5897/ajb12.1043.
8. L. C. Razanamahandry, A. C. Nwanya, M. O. Akharame, B. U. Muhammad, S. K. O. Ntwampe, and E. Fosso-Kankeu, "Recovery of iron nanoparticles from mine wastewater using plant extracts of Eucalyptus Globulus, Callistemon Viminalis and Persea Americana," Minerals, vol. 10, no. 10, pp. 1–15, 2020, doi: 10.3390/min10100859.
9. S. Ilari et al., "Protective effect of antioxidants in nitric oxide/COX-2 interaction during inflammatory pain: the role of nitration," Antioxidants, vol. 9, no. 12, p. 1284, 2020.
10. H. L. Hsieh and C. M. Yang, "Role of redox signaling in neuroinflammation and neurodegenerative diseases," Biomed Res. Int., vol. 2013, 2013, doi: 10.1155/2013/484613.
11. R. Nørregaard, T.-H. Kwon, and J. Frøkiær, "Physiology and pathophysiology of cyclooxygenase-2 and prostaglandin E2 in the kidney," Kidney Res. Clin. Pract., vol. 34, no. 4, pp. 194–200, 2015.
12. M. S. H. Bhuiyan et al., "Green synthesis of iron oxide nanoparticle using Carica papaya leaf extract: application for photocatalytic degradation of remazol yellow RR dye and antibacterial activity," Heliyon, vol. 6, no. 8, p. e04603, 2020, doi: 10.1016/j.heliyon.2020.e04603.
13. K. M. Ibrahim, R. K. Naem, and A. S. Abd-Sahib, "Antibacterial activity of nutmeg (Myristica fragrans) seed extracts against some pathogenic bacteria," Al-Nahrain J. Sci., vol. 16, no. 2, pp. 188–192, 2013.
14. K. M. Ibrahim, R. K. Naem, and A. S. Abd-Sahib, "Antibacterial Activity of Nutmeg (Myristica fragrans) Seed Extracts Against Some Pathogenic Bacteria," J. Al-Nahrain Univ. Sci., vol. 16, no. 2, pp. 188–192, 2013, doi: 10.22401/jnus.16.2.29.
15. K. A. L. I. DEHGHAN, I. Rasooli, M. B. Rezaee, and P. Owlia, "Antioxidative properties and toxicity of white rose extract," 2011.

16. I. E. Juárez-Rojop, C. A. Tovilla-Zárate, and D. E. Aguilar-Domínguez, “Roade la Fuente LF, Lobato-García CE, Blé-Castillo JL, López-Meraz L, Díaz-Zagoya JC, Bermúdez-Ocaña DY. Phytochemical screening and hypoglycemic activity of Carica papaya leaf in streptozotocin-induced diabetic rats,” Rev. Bras. Farmacogn., vol. 24, pp. 341–347, 2014.
17. B. Ahmmad et al., “Green synthesis of mesoporous hematite (α-Fe2O 3) nanoparticles and their photocatalytic activity,” Adv. Powder Technol., vol. 24, no. 1, pp. 160–167, 2013, doi: 10.1016/j.apt.2012.04.005.
18. H. S. Devi, M. A. Boda, M. A. Shah, S. Parveen, and A. H. Wani, “Green synthesis of iron oxide nanoparticles using Platanus orientalis leaf extract for antifungal activity,” Green Process. Synth., vol. 8, no. 1, pp. 38–45, 2019, doi: 10.1515/gps-2017-0145.
19. M. Khan et al., “Plant extracts as green reductants for the synthesis of silver nanoparticles: Lessons from chemical synthesis,” Dalt. Trans., vol. 47, no. 35, pp. 11988–12010, 2018.
20. V. C. Karade et al., “A green approach for the synthesis of α-Fe2O3 nanoparticles from Gardenia resinifera plant and it’s In vitro hyperthermia application,” Heliyon, vol. 5, no. 7, p. e02044, 2019.
21. C. Mystrioti, T. D. Xanthopoulou, P. Tsakiridis, N. Papassiopi, and A. Xenidis, “Comparative evaluation of five plant extracts and juices for nanoiron synthesis and application for hexavalent chromium reduction,” Sci. Total Environ., vol. 539, pp. 105–113, 2016.
22. S. O. Aisida et al., “Biogenic synthesis of iron oxide nanorods using Moringa oleifera leaf extract for antibacterial applications,” Appl. Nanosci., vol. 10, no. 1, pp. 305–315, 2020, doi: 10.1007/s13204-019-01099-x.
23. W. J. Aziz, M. A. Abid, D. A. Kadhim, and M. K. Mejbel, “Synthesis of iron oxide (β-fe2o3) nanoparticles from Iraqi grapes extract and its biomedical application,” IOP Conf. Ser. Mater. Sci. Eng., vol. 881, no. 1, 2020, doi: 10.1088/1757-899X/881/1/012099.
24. E. Üstün, S. C. Önbaş, S. K. Çelik, M. Ç. Ayvaz, and N. Şahin, “Green synthesis of iron oxide nanoparticles by using ficus carica leaf extract and its antioxidant activity,” Biointerface Res. Appl. Chem., vol. 12, no. 2, pp. 2108–2116, 2022, doi: 10.33263/BRIAC122.21082116.
25. E. Rostamizadeh, A. Iranbakhsh, A. Majd, S. Arbabian, and I. Mehregan, “Green synthesis of Fe2O3 nanoparticles using fruit extract of Cornus mas L. and its growth-promoting roles in Barley,” J. Nanostructure Chem., vol. 10, no. 2, pp. 125–130, 2020, doi: 10.1007/s40097-020-00335-z.
26. T. Shahwan et al., “Green synthesis of iron nanoparticles and their application as a Fenton-like catalyst for the degradation of aqueous cationic and anionic dyes,” Chem. Eng. J., vol. 172, no. 1, pp. 258–266, 2011.
27. S. Bhattacharya, I. Saha, A. Mukhopadhyay, D. Chattopadhyay, and U. Chand, “Role of nanotechnology in water treatment and purification: Potential applications and implications,” Int. J. Chem. Sci. Technol., vol. 3, no. 3, pp. 59–64, 2013.
28. I. Bibi et al., “Green synthesis of iron oxide nanoparticles using pomegranate seeds extract and photocatalytic activity evaluation for the degradation of textile dye,” J. Mater. Res. Technol., vol. 8, no. 6, pp. 6115–6124, 2019, doi: 10.1016/j.jmrt.2019.10.006.
29. S. Kanagasubbulakshmi and K. Kadirvelu, “Green synthesis of Iron oxide nanoparticles using Lagenaria siceraria and evaluation of its Antimicrobial activity,” Def. Life Sci. J., vol. 2, no. 4, p. 422, 2017, doi: 10.14429/dlsj.2.12277.
30. V. G. Viju Kumar and A. A. Prem, “Green synthesis and characterization of iron oxide nanoparticles using phyllanthus niruri extract,” Orient. J. Chem., vol. 34, no. 5, pp. 2583–2589, 2018, doi: 10.13005/ojc/340547.

31. S. Suresh, S. Karthikeyan, and K. Jayamoorthy, “Effect of bulk and nano-Fe2O3 particles on peanut plant leaves studied by Fourier transform infrared spectral studies,” J. Adv. Res., vol. 7, no. 5, pp. 739–747, 2016.

32. A. Lassoued, M. S. Lassoued, B. Dkhil, S. Ammar, and A. Gadri, “RETRACTED ARTICLE: Photocatalytic degradation of methylene blue dye by iron oxide (α-Fe 2 O 3) nanoparticles under visible irradiation,” J. Mater. Sci. Mater. Electron., vol. 29, no. 10, pp. 8142–8152, 2018.

33. C. H. Ramamurthy et al., “The extra cellular synthesis of gold and silver nanoparticles and their free radical scavenging and antibacterial properties,” Colloids Surfaces B Biointerfaces, vol. 102, pp. 808–815, 2013, doi: 10.1016/j.colsurfb.2012.09.025.

34. J. Asgarpanah and N. Kazemivash, “Phytochemistry and pharmacologic properties of Myristica fragrans Hoyutt.: A review,” African J. Biotechnol., vol. 11, no. 65, pp. 12787–12793, 2012.

35. A. K. Mittal, J. Bhaumik, S. Kumar, and U. C. Banerjee, “Biosynthesis of silver nanoparticles: Elucidation of prospective mechanism and therapeutic potential,” J. Colloid Interface Sci., vol. 415, pp. 39–47, 2014, doi: 10.1016/j.jcis.2013.10.018.

36. H. E. A. Mohamed et al., “Bio-redox potential of Hyphaene thebaica in bio-fabrication of ultrafine maghemite phase iron oxide nanoparticles (Fe2O3 NPs) for therapeutic applications,” Mater. Sci. Eng. C, vol. 112, no. March, p. 110890, 2020, doi: 10.1016/j.msec.2020.110890.

37. C. López-Alarcón and A. Denicola, “Evaluating the antioxidant capacity of natural products: A review on chemical and cellular-based assays,” Anal. Chim. Acta, vol. 763, pp. 1–10, 2013, doi: 10.1016/j.aca.2012.11.051.

38. H. Dorman and S. G. Deans, “Antimicrobial agents from plants: antibacterial activity of plant volatile oils,” J. Appl. Microbiol., vol. 88, no. 2, pp. 308–316, 2000.

39. E. Ceylan and D. Y. C. Fung, “Antimicrobial activity of spices 1,” J. Rapid Methods Autom. Microbiol., vol. 12, no. 1, pp. 1–55, 2004.

40. Z. Luo, Y. Qin, and Q. Ye, “Effect of nano-TiO2-LDPE packaging on microbiological and physicochemical quality of Pacific white shrimp during chilled storage,” Int. J. Food Sci. Technol., vol. 50, no. 7, pp. 1567–1573, 2015.

41. P. Jaiswal et al., “ARBS Annual Review of Biomedical Sciences Biological Effects of Myristica fragrans,” ARBS Annu. Rev. Biomed. Sci., pp. 21–29, 2009.

42. A. Takikawa et al., “Antimicrobial activity of nutmeg against Escherichia coli O157,” J. Biosci. Bioeng., vol. 94, no. 4, pp. 315–320, 2002.

43. P. Rani and N. Khullar, “Antimicrobial evaluation of some medicinal plants for their anti-enteric potential against multi-drug resistant Salmonella typhi,” Phyther. Res. An Int. J. Devoted to Pharmacol. Toxicol. Eval. Nat. Prod. Deriv., vol. 18, no. 8, pp. 670–673, 2004.